Simulation of resonance scattering helioseismometer signals from spatially resolved images: Application to the GOLF instrument on SOHO

R.K. Ulrich[1], P. Boumier[2], J.-M. Robillot[3], R.A. García[4], T. Roca Cortés[5], and C.J. Henney[6]

[1] UCLA, Department of Physics & Astronomy, Los Angeles, CA 90095-1562, USA
[2] Institut d'Astrophysique Spatiale, Orsay, France
[3] Observatoire de l'Université de Bordeaux I, Bordeaux, Floirac, France
[4] Service d'Astrophyique, C.E.A., Saclay, France
[5] Instituto de Astrofísica de Canarias, 38205 La Laguna, Tenerife, Spain
[6] National Solar Observatory, 950 North Cherry Avenue, Tucson, AZ 85726-6732, USA

Abstract. A step in the analysis of the data from the GOLF (Global Oscillations at Low Frequency) instrument on SOHO (SOlar and Heliospheric Observatory, an ESA/NASA Mission) involves the calculation of the sensitivity of the GOLF signal to the velocity at each point on the solar surface. A successful model of this sort will permit the intercomparison of data from the spatially resolved MDI (Michelson Doppler Imager) instrument to the integrated sunlight GOLF signal. This paper presents a formalism and data adequate for the calculation of the required sensitivity functions. An important complication in the treatment of the GOLF data is the need to include both the sodium D_1 and D_2 lines. The latter is subject to contamination by telluric absorption and is difficult to observe from ground-based systems. This paper presents some telluric corrected data for the D_2 line. The uniform displacement of the solar surface is an important special case which is observed directly by GOLF. The comparison of the appropriate integral of the sensitivity function derived from the ground-based profiles to that derived from GOLF data shows that the model can successfully reproduce important properties of the GOLF instrument function. A formalism and some data are presented which allow the calculation of the sensitivity of the GOLF instrument to magnetic effects. At present this approach takes a form in which the full magnetic effect is approximated by the magnetic effect on the sodium D_1 line alone.

Key words: Sun: atmosphere – Sun: oscillations

1. Introduction

The Global Oscillations at Low Frequency (GOLF) instrument on board the ESA/NASA sponsored Solar and Heliospheric Observatory (SOHO) measures solar velocities in integrated sun-

light using a sodium resonance scattering system. Details of the instrument and its initial results have been given by Gabriel et al. (1995, 1997). A series of papers describing the conversion of the instrument signal into a quantity related to velocity is in preparation (García et al. 2000, Ulrich et al. 2000). Preliminary reports of these studies have been given by Ulrich et al. (1998) and Robillot et al. (1998). This paper describes an extension of the integrated sunlight analysis to an analysis of the dependence of the integrated signal on spatially resolved velocities such as can be obtained from the Michelson Doppler Imager (MDI) instrument which is also on board SOHO.

The formalism presented in this paper is applied to the GOLF instrument operating in the single-wing mode. The extension to similar instruments in dual or multiple wing modes is straightforward and indeed the original version of this model was intended for application to GOLF operations in the two-wing mode. At a fundamental level, one would wish to track the effect of a velocity displacement of the solar surface through to a signal detected by some instrument like those on SOHO. Intermediary effects include the displacement of spectral lines, the alteration of line profiles and changes in the continuum intensity. In addition, one would like to understand the effects of non-velocity perturbations such as might be caused by magnetic fields. Although it is possible to estimate the magnitude of such effects and we provide here a set of functions which allow their estimation, there is no possibility of compensating for them in the GOLF signal unless there is a data set providing a magnetically sensitive parameter on essentially the same time base as is available for the GOLF data. Although one parameter from the MDI instrument, the line strength parameter, is recorded as part of the MDI structure program, up to this time it has not been used thus far as a tool for the study of magnetic effects in the GOLF data. As a first step we concentrate on the effect of spectral line shift as the mechanism which produces the dominant signal in velocity sensitive instruments and report

an approximate approach which can be used for the treatment of data during periods of high solar activity.

The need for a detailed understanding of the sensitivity of an integrated-sunlight instrument like GOLF to the spatial distribution of line-of-sight velocities over the solar surface comes from the advantages to be gained through the intercomparison of signals from several instruments. In the case of the helioseismology instruments on SOHO, our objective is to prepare data sets from the GOLF and MDI instruments which most closely resemble each other so that the different effects of solar noise in the two instrument data streams can be reduced by means of a cross-correlation technique. Our approach does not aim for an exact reproduction of the GOLF signal from the MDI images since both contain contributions from the largely random convective processes. Rather we seek to maximize the common coherent components of each so that the cross correlation method can achieve its best possible performance. The height of formation of the spectral lines used by GOLF and MDI differs with the Ni line used by MDI being formed closer to the photosphere than the points on the Na line used by GOLF. Because signals due to convection are a stronger function of height in the solar atmosphere than the coherent, global oscillations, we can enhance our ability to distinguish between these processes by carefully determining the spatial weighting function to be applied to the resolved data in order to create a simulation of the integrated sunlight signal. Indeed, results from this approach, which include the identification of modes having frequencies as low as 535.75 μHz, are described in a series of papers (Henney 1999, Henney et al. 1999, Bertello et al. 2000a, 2000b). An ultimate goal from an approach like ours would be to determine a convective and active region signal from spatially resolved observations by MDI and subtract this signal from the GOLF signal. We refer to such an approach as a signal subtraction method as opposed to the signal cross-correlation method which we use. If the method works, the rms variation in the subtracted signal should be less than that in either of the time series forming the difference. Unfortunately due to the combined effects of shutter noise in the MDI instrument and the single wing mode of operation by GOLF, the signal subtraction method was not successful in our studies.

A similar analysis of instrument sensitivity has been given by Christensen-Dalsgaard (1989) and applied to the instrument configurations of the IRIS and BISON systems. That analysis did not include the treatment of multiple components necessary for the GOLF system nor did it include explicitly measured center to limb effects on the line profile nor did it use explicitly measured differential rotation and limb shift factors appropriate to the Na D lines. In another simulation study García, Roca Cortés and Régulo (1998) have used an approach similar to that by Christensen-Dalsgaard (1989) to calculate the response of the GOLF instrument to two 12-month series of simulated solar velocity fields. This study represented the solar D lines as gaussians whose slopes in the spectral range covered during GOLF operations differ substantially from those of the solar D lines, and did not use limb darkening, limb shift and solar rotation curves appropriate for the D lines. This formulation

has not been used with actual solar data from MDI so we cannot determine the effects of these approximations on our ability to carry out the cross-correlation analysis. While these details do not alter the overall nature of the sensitivity functions derived by Christensen-Dalsgaard (1989) and García, Roca Cortés and Régulo (1998), the unique opportunity presented by the space-based helioseismology instruments on SOHO requires that we treat the observations using the best possible model. This paper is one step in that process.

Although the focus of the present work is to describe the sensitivity of the GOLF instrument to velocity variations on the solar surface, additional functions needed to describe the sensitivity of the GOLF instrument to magnetic effects are defined and evaluated in an approximate fashion here. While the method can be extended by the evaluation of these additional terms using additional data to include the effects of active regions, magnetic data of adequate precision and with appropriate temporal and spatial resolution has not yet been extracted from the available instrument systems to permit an application of these terms to the correction of the GOLF time series. Consequently, we concentrate in this and subsequent papers on the spectral band between 200 and 1000 μHz where the active region induced signal is only a fraction of the total non-coherent variations. The GOLF signal used in this series of papers is obtained with the method described by Ulrich et al. (2000). As obtained from this method, the shape of the solar background power spectrum makes it clear that in the 200-1000 μHz range the solar noise is not dominated by the active region effects. Further discussion of the inter-relationships between solar signals, the signal subtraction method, global modes of solar oscillation and the GOLF and MDI instruments is given in the conclusions.

We seek here a function of position on the solar disk which when multiplied pointwise with the velocity on the solar disk will yield the change in the signal detected by GOLF. We call this the sensitivity function. For the case of a single scattering component in a spectral line, conceptually this sensitivity function is the difference between two spectroheliogram images taken through extremely narrow band-pass filters whose wavelengths bracket the working point of the GOLF instrument. An imaging system utilizing a sodium vapor cell as a band-pass filter which included a modulated magnetic field could obtain such images directly. However, there is at present no such system nor could there be a ground-based system measuring both the D_1 and D_2 lines simultaneously due to the problems of telluric contamination. Thus we have to approach this task indirectly utilizing available observing systems.

To model the system indirectly we note that it is possible to factor the sensitivity function into parts which are separately measurable with existing instrument systems: a line profile function and a center-to-limb intensity function. Line profiles are normally given as a ratio of the monochromatic intensity to the continuum intensity. Since only the product of these two functions is needed, we show here that the line bisector intensity can be used in place of the continuum intensity in defining the line profile and its slope at the GOLF working points. Since a Babcock (1953) magnetograph such as the one in use at the

150-foot solar tower on Mt. Wilson normally keeps the spectral line centered between its blue and red spectral sampling ports, the measured average intensity is inherently a bisector intensity. Thus if we reference the line profile to the bisector point defined by the Babcock magnetograph, utilize the center-to-limb bisector intensity from the magnetograms with a matching blue and red spectral port separation, and utilize a rotation and limb shift function appropriate to the spectral line in question, we can combine the two forms of data to recover the desired sensitivity function. Line profile functions are needed at several points on the solar surface and they can be measured with the facilities of the MWO 150-foot solar tower (Ulrich et al. 1991, 1993). Furthermore, we can obtain the measurements needed for all the components of the D lines and combine the sensitivity functions according to the measured scattering strength to obtain a net sensitivity function for the GOLF instrument.

The utilization of the Babcock magnetograph data and the line profile data for the analysis of the GOLF signal from both D_1 and D_2 lines requires the development of a notation which can clearly deal with multiple components. This notation is described in the next section. The Mt. Wilson line profiles are presented and described in Sect. 3. Next the velocities and limb darkening functions derived from the magnetograph observations are presented in Sect. 4. Finally the sensitivity functions are derived in Sect. 5 and compared to the integrated sensitivity function derived directly from GOLF.

2. The GOLF signal

The sensitivity of the GOLF signal has recently been discussed by García et al. (2000) and Ulrich et al. (1998, 2000). Details of the system in terms of the magnetic field configuration, the properties of the scattering cell and the resultant scattering strengths are found in those papers. The objective of this paper is to evaluate solar factors which influence the GOLF measurement. There could be additional factors due to the instrument which might influence the signal dependence on position over the solar disk. During the commissioning phase of SOHO, the spacecraft performed off-set pointing tests which altered the optical path of the sunlight through the instrument. During these tests there was no detectable change in the GOLF signal (Gabriel et al. 1997). This off-set pointing performance demonstrates that there is no vignetting in the system and that the instrument responds uniformly to all parts of the solar disk. This performance is a result of the high degree of uniformity of the magnetic field in the scattering portion of the cell and the fact that the temperature of the scattering gas is sufficiently low that self-absorption within the cell is not a factor. The only instrument thermal effect which influences the spatial characteristics of the instrument response is that due to the cell temperature which changes the balance between the three scattering components. This temperature variation effect is included in the model. Other instrumental variations alter the overall gain of the signal but do not alter the spatial characteristics. For example, it has been hypothesized by Ulrich et al. (2000) that an interference fringe in one of the blocking filters is evolving and producing a sinusoid-like time

dependence in the instrument throughput. Such a fringe could also introduce a wavelength and velocity dependent factor which might alter the spatial response. However, this effect is ruled out by comparison of the phase of the sinusoid-like function in the two states of magnetic modulation. No phase difference was detectible. Based on such considerations, we do not consider any instrumental factors as significant apart from those discussed below.

The discussion in this paper follows the formalism presented in the above earlier papers and extends that treatment to the case of a spatially resolved image. The GOLF instrument system utilizes both D_1 and D_2 lines. Telluric absorption components near the working point on the red wing of D_2 complicate ground-based studies of this line. Since both members of the doublet are scattered into the detection chain, there are three separate wavelength bands combined to yield a single signal for every configuration of the GOLF instrument. We designate these components as λ_1, λ_{2a} and λ_{2b}. These longitudinal Zeeman components are offset from the non-magnetic wavelengths $\lambda_{0,1} = 589.5924$ nm and $\lambda_{0,2a} = \lambda_{0,2b} = 588.9950$ nm (Reader & Corliss 1980) to wavelengths of

$$\begin{aligned}
\lambda_{b,i}^{\pm} &= \lambda_{0,i} - g_i(\Delta\lambda_B \pm \delta\lambda_B) \\
\lambda_{r,i}^{\pm} &= \lambda_{0,i} + g_i(\Delta\lambda_B \pm \delta\lambda_B)
\end{aligned} \tag{1}$$

where GOLF's permanent magnetic field strength B_0 is 5040 ± 40 gauss and there is an additional variable field coming from an electromagnet whose modulation amplitude is $\delta B = 76.9\pm1$ gauss. Thus the wavelength increments are:

$$\Delta\lambda_B = A\,B_0 \quad , \quad \delta\lambda_B = A\delta B \tag{2}$$

with Zeeman factors of

$$(g_1, g_{2a}, g_{2b}) = (4/3, 5/3, 3/3) . \tag{3}$$

Following Boumier (1991) we have used the notation $i = 1, 2a, 2b$ to designate these components respectively. The precision of the above determination of the modulation amplitude applies to the offset in GOLF signal obtained during the two-wing period of operation and represents the shift necessary to yield equal line of sight velocity for two different combinations of intensity. The actual magnetic field in the instrument could be different. However, the determined parameter is the quantity which influences the analysis of the GOLF data according to the methods outlined here and it is well determined as indicated by the above quoted errors. The magnetic conversion factor A is 1.62×10^{-6} for magnetic fields in gauss and wavelengths in nm and we have neglected a small difference in the value of A for the D_1 and D_2 lines.

Following the notation of Ulrich et al. (2000) we distinguish between a realized intensity and a line profile function by representing the intensities as in a mathitalic notation such that for example I_b^+ refers to the intensity in the blue wing with the positive state of the electromagnet. For a line profile function we use bold face and explicitly indicate the input quantity on which it depends: $\boldsymbol{I}_{\lambda,j}\{w, \rho, B\}$ is such a profile function for spectral line j depending on w which has dimensions of wavelength. We have explicitly indicated that the profile function depends

on center-to-limb angle ρ and surface magnetic field strength B. In our case w is the wavelength difference between the scattering component at wavelength λ and a centroid of the solar line at wavelength $\lambda_\odot$. Each solar line profile $\boldsymbol{I_{\lambda,j}}\{\lambda - \lambda_\odot, \rho, B\}$ may depend on other parameters such as position within a supergranule cell. At present we use the profiles described in the following section and neglect this variation as well as that due to B so that they can be taken as a constant when averaged over long time periods.

The GOLF instrument selects the solar radiation by resonance scattering from the sodium atoms within a heated cell in a strong magnetic field. The scattering strength depends on cell temperature and the magnetic field structure and is represented here by a scattering function ϕ_i for each of the scattering components. These functions are given by Boumier & Damé (1993). The signals observed by GOLF are then:

$$I_b^\pm = \sum_i \phi_i \int\limits_{\mathrm{Surf}} \boldsymbol{I_{\lambda,j}}\{\lambda_{b,i}^\pm - \lambda_\odot(x,y), \rho\}dx\,dy \quad (4)$$

$$I_r^\pm = \sum_i \phi_i \int\limits_{\mathrm{Surf}} \boldsymbol{I_{\lambda,j}}\{\lambda_{r,i}^\pm - \lambda_\odot(x,y), \rho\}dx\,dy \quad (5)$$

which yield:

$$I_b^\pm = \sum_i \phi_i \times$$
$$\int\limits_{\mathrm{Surf}} \boldsymbol{I_{\lambda,j}}\Big\{ - g_i(\Delta\lambda_B \pm \delta\lambda_B) - \lambda_0 \frac{v(x,y)}{c}, \rho \Big\}dx\,dy \quad (6)$$

$$I_r^\pm = \sum_i \phi_i \times$$
$$\int\limits_{\mathrm{Surf}} \boldsymbol{I_{\lambda,j}}\Big\{ + g_i(\Delta\lambda_B \pm \delta\lambda_B) - \lambda_0 \frac{v(x,y)}{c}, \rho \Big\}dx\,dy \quad (7)$$

where the intensity $\boldsymbol{I_{\lambda,j}}$ includes the limb darkening which is the indicated function of ρ and the velocity $v(x,y)$ which is the total doppler shift of a point at coordinates (x,y) due to the Einstein gravitation red shift, the orbital sun-spacecraft velocity, the differential rotation and the convective limb shift effect. The (x,y) coordinate system is rectangular in the plane of the sky and can have a zero point defined to be at the solar disk center. The dimensions of x and y need to be consistent with those for $R_\odot$ for the purpose of normalizing various integrals.

Eqs. (6) and (7) require knowledge of the line profiles over some range in v near each of the working points. For the full velocity range of the orbital motion of SOHO, the line profiles are significantly non-linear. For the purpose of the determination of the velocity sensitivity, we may consider a restricted range in which case the profile is nearly linear. We may then define a reference velocity v_{ref} and consider $\delta v = v - v_{\mathrm{ref}}$ to be small. The magnetic field and its modulation correspond to the velocity shifts:

$$\Delta v_B = c\Delta\lambda_B/\lambda_0 = (cA/\lambda_0)\Delta B \quad (8)$$
$$\delta v_B = c\delta\lambda_B/\lambda_0 = (cA/\lambda_0)\delta B \,. \quad (9)$$

We may also remap the functional form of the line profile so that the input parameter is $v = -(c/\lambda_0)w$ instead of wavelength w: $\boldsymbol{I_{v,j}}\{ -(c/\lambda_0)w \} = \boldsymbol{I_{\lambda,j}}\{w\}$. After adopting the following compact notation for the derivative with respect to velocity:

$$\boldsymbol{I'_{v,j}} = \frac{d\boldsymbol{I_{v,j}}}{dv} = -\frac{\lambda_0}{c}\frac{d\boldsymbol{I_{\lambda,j}}}{d\lambda} \quad (10)$$

and defining:

$$I_{b,i}^\pm(x,y) = \boldsymbol{I_{v,j}}\{ -g_i(\Delta v_B \pm \delta v_B) - v_{\mathrm{ref}}(x,y) \}, \quad (11)$$
$$I_{r,i}^\pm(x,y) = \boldsymbol{I_{v,j}}\{ +g_i(\Delta v_B \pm \delta v_B) - v_{\mathrm{ref}}(x,y) \}, \quad (12)$$
$$\Big(I_{b,i}^\pm(x,y)\Big)'_v = \boldsymbol{I'_{v,j}}\{ -g_i(\Delta v_B \pm \delta v_B) - v_{\mathrm{ref}}(x,y) \}, \quad (13)$$
$$\Big(I_{r,i}^\pm(x,y)\Big)'_v = \boldsymbol{I'_{v,j}}\{ +g_i(\Delta v_B \pm \delta v_B) - v_{\mathrm{ref}}(x,y) \} \quad (14)$$

and using a linear expansion about the reference velocity we obtain:

$$I_b^\pm(x,y) = \sum_i \phi_i \left[I_{b,i}^\pm(x,y) + \Big(I_{b,i}^\pm(x,y)\Big)'_v \delta v(x,y) \right], \quad (15)$$

$$I_r^\pm(x,y) = \sum_i \phi_i \left[I_{r,i}^\pm(x,y) + \Big(I_{r,i}^\pm(x,y)\Big)'_v \delta v(x,y)) \right]. \quad (16)$$

Two properties of these definitions are worth emphasizing: first, even though we have used a velocity scale for the argument of the line profile function, we have reversed the sign in order to account for the fact that the velocity appears with a negative sign in Eqs. (11 - 14); and second, the slopes $(I_{b,i}(x,y))'_v$ are positive while the slopes $(I_{r,i})'_v$ are negative.

3. The Mt. Wilson line profiles

The Na line profiles used to model the GOLF velocity sensitivity functions were observed at the Mt. Wilson 150-ft solar tower (e.g. Ulrich et al. 1991). The Na D_1 and D_2 profiles were observed at three disc positions: 0, 60 and 75 degrees. Additional sets of data are available at 45 degrees for D_1 and 30 degrees for D_2. These were well represented by linear interpolation between 0 and 60 degrees and since they corresponded to different center-to-limb angles it was determined to leave them out of the interpolation table and simply use linear interpolation between 0 and 60 degrees for both lines. Linear interpolation and extrapolation was also used for all angles greater than 60 degrees using the measurements at 60 and 75 degrees. The sampling of the solar surface can be carried out in a variety of ways as was described by Ulrich et al. (1991). For the scans of D_1, the entrance aperture used was plain slit (no Walraven Image Slicer). The sampled area in these cases was 1 arc-second by 20 arc-seconds. For the D_2 scans, the Walraven Image slicer was left in place and an aperture of 12 arc-seconds by 12 arc-seconds was used. Comparisons between profiles of the D_1 line profile made with these different configurations show that the changes due to solar conditions are larger than those caused by the optical configuration. The average line profiles obtained with this system are formed out of 180 separate scans each of which requires 30 seconds of time. As each scan is added to
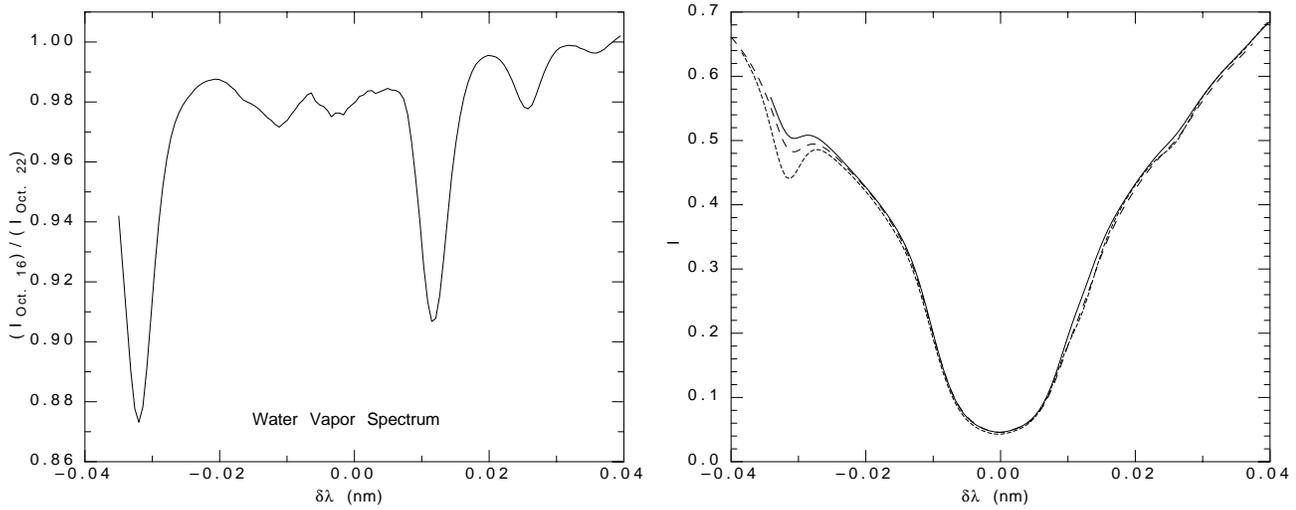
Fig. 1. The Na D_2 water vapor absorption spectrum (left) as observed from the Mt. Wilson 150-ft solar tower. The water vapor spectrum is derived from the ratio of the D_2 profiles observed with the strongest and weakest absorption features shown in the right panel.

the sum, it is first shifted so that its line bisector at ± 10 pm (10 picometers= 100 mÅ) coincides with those already in the sum. In this way, the smearing effect of the 5-minute oscillations is largely removed. The instrumental smearing due to spectral resolution is equivalent to convolving the true solar profile with a gaussian having a half-width of 3 pm. This is larger than the smearing caused by the GOLF instrument itself (Boumier & Damé 1993) but is comparable to the smearing caused by short wavelength surface velocity fields.

The D_2 line is strongly affected by telluric water absorption at wavelengths of interest for modeling the GOLF response. The water vapor is distributed somewhat irregularly through the atmosphere and is time variable during the observing day so that the absorption components introduced by this species cannot be assumed to follow a secant of the zenith angle law. During the months of October to December of 1995, the D_2 line was measured at the Mt. Wilson 150-foot solar tower on a regular basis for about one hour near local noon. Due to the above noted variability of the column depth of water vapor in the earth's atmosphere, the telluric features vary considerably in strength from one observation to the next. Initially the data was obtained at disk center in order to learn the nature of the telluric features as observed by the Mt. Wilson system. A set of three days has been selected as representing a considerable range in these features. These are Oct. 22 with the weakest features, Oct. 14 with intermediate strength features and Oct. 16 with the strongest features. The ratio of the spectrum for Oct. 16 to that for Oct. 22 is shown in the left panel of Fig. 1. The right panel of Fig. 1 shows these three line profiles. The effect of the telluric absorption was removed by multiplying the observed intensity by $\exp(\tau_\lambda^{\mathrm{Tell}})$. The telluric optical depth was modeled as the sum of four gaussians: $\tau_\lambda^{\mathrm{Tell}} = A \sum_i^4 a_i \exp\left[-0.5(\frac{\lambda - \lambda_i}{\sigma})^2\right]$ where the width $\sigma = 2.1$ pm was adopted at wavelengths of -32.30, -1.13, 11.30 and 25.35 pm relative to the D_2 line center. The apparent feature at -12 pm was omitted as it appeared from other line pairs to be a result of a line profile change rather than telluric absorption.

The relative amplitudes a_i of the components were taken to be $\{1.0, 0.1, 0.8, 0.18\}$. The nominal line center wavelength and the overall scale factor A were adjusted to provide a smooth profile at wavelengths near the strongest feature at -32.30 pm. When the profile in this wing was relatively smooth, the features at wavelengths of greater interest also largely vanish. The D_1 lines did not require a correction of this type. Each line profile is corrected for the effect of spectral resolution by deconvolving with an instrumental function derived from the ratio of the line profile measured when the sunlight traverses a hot sodium cell to the profile without the sodium absorption. The profiles are also corrected for the effect of spectrograph scattered light which introduces a constant offset equivalent to 2% of continuum. The resulting corrected line profiles are shown in Fig. 2.

The line profile system described by Ulrich et al. (1991) operates by scanning a fiber-optic aperture in alternating directions over the spectral image at the focal point of the Littrow lens. The final scans are formed out of averages of 120 to 150 of the subscans. The scanning process is controlled by a precision motor which has a maximum translation speed. The requirement of finishing each subscan in less than 30 seconds in order to properly sample the 5-minute oscillations imposes a limit on the wavelength coverage of the profiles. Consequently, the Mt. Wilson profiles do not extend to the continuum. However, as long as the relative intensity over the full solar disk can be measured at the GOLF working points, there is no need to know the continuum intensity. During normal magnetograph operation at the Mt. Wilson 150-foot solar tower, the average intensity at points on opposite sides of the solar line is mapped over the full solar surface. This intensity corresponds to the line bisector intensity and the quantity we require is the limb darkening function for the bisector whose blue and red sampling points are separated in wavelength by an amount the same as the physical separation of the magnetograph blue and red line wing sampling optics. The shifted intensity resulting from a velocity difference between the bisector and an arbitrarily moving part of the solar
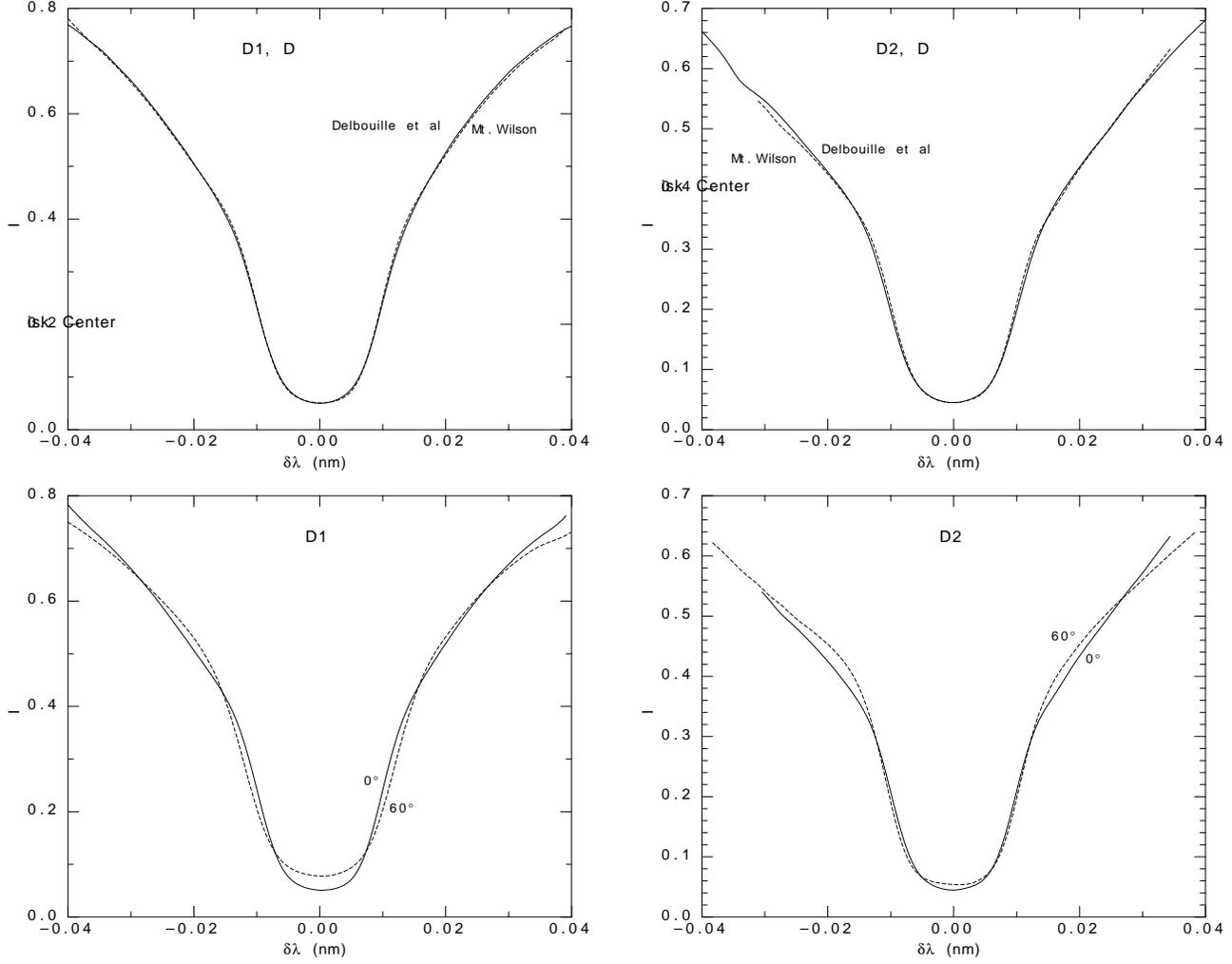
Fig. 2. Na D line profiles observed from the Mt. Wilson 150-ft solar tower compared to the Debouille et al. (1973) profiles (upper panels). In addition, the Na D profiles observed at disk center and $\rho= 60$ (lower panels).

surface adds a correction to this bisector velocity which can be calculated from knowledge of the line profiles as a function of position on the solar surface.

4. The magnetograph velocities and center-to-limb intensity curves

In order to evaluate surface integrals of Eqs. (6) and (7) we need to know the velocity function $v(x, y)$ and we need to know how the intensity depends on center-to-limb position. The magnetograph system provides a direct way to obtain both these quantities. The essential feature of the system is that it automatically tracks the bisector position. Thus the magnetogram velocity map gives us the shift of the bisector and the limb darkening curve gives us the appropriate intensity of this bisector. The parameter defining the bisector as measured by the magnetograph is the separation $2\Delta_i^{\pm}$ between the wavelengths where the intensity is balanced. There are six values of $\Delta_i^{\pm}$ we need to use, one for each phase of magnetic modulation for each of the three scattering com-

ponents. These values are: $(\Delta_1^-, \Delta_1^+, \Delta_{2a}^-, \Delta_{2a}^+, \Delta_{2b}^-, \Delta_{2b}^+) = (10.72, 11.09, 13.44, 13.68, 8.06, 8.32)$ pm.

We must define a velocity and intensity system relative to the above bisectors. At the bisector, the quantity $v_{\rm ref}$ of Eqs. (11) to (14) is zero. The value of $v_{\rm ref}(x, y)$ then is the desired long-time average offset velocity of a pixel at position (x, y) on the solar image. The average intensity of this pixel can then be expressed as the product of the bisector intensity

$$
\begin{aligned}
I_{\Delta_i^{\pm}} &= \boldsymbol{I_{v,j}} \left\{ + g_i(\Delta v_B \pm \delta v_B) \right\} \\
&= \boldsymbol{I_{v,j}} \left\{ - g_i(\Delta v_B \pm \delta v_B) \right\}
\end{aligned}
\tag{17}
$$

and a line profile ratio

$$
q_{i,b,\Delta_i^{\pm}}(v_{\rm ref}) = \frac{\boldsymbol{I_{v,j}} \left\{ - g_i(\Delta v_B \pm \delta v_B) - v_{\rm ref} \right\}}{\boldsymbol{I_{v,j}} \left\{ - g_i(\Delta v_B \pm \delta v_B) \right\}}
\tag{18}
$$

$$
q_{i,r,\Delta_i^{\pm}}(v_{\rm ref}) = \frac{\boldsymbol{I_{v,j}} \left\{ + g_i(\Delta v_B \pm \delta v_B) - v_{\rm ref} \right\}}{\boldsymbol{I_{v,j}} \left\{ + g_i(\Delta v_B \pm \delta v_B) \right\}}
\tag{19}
$$

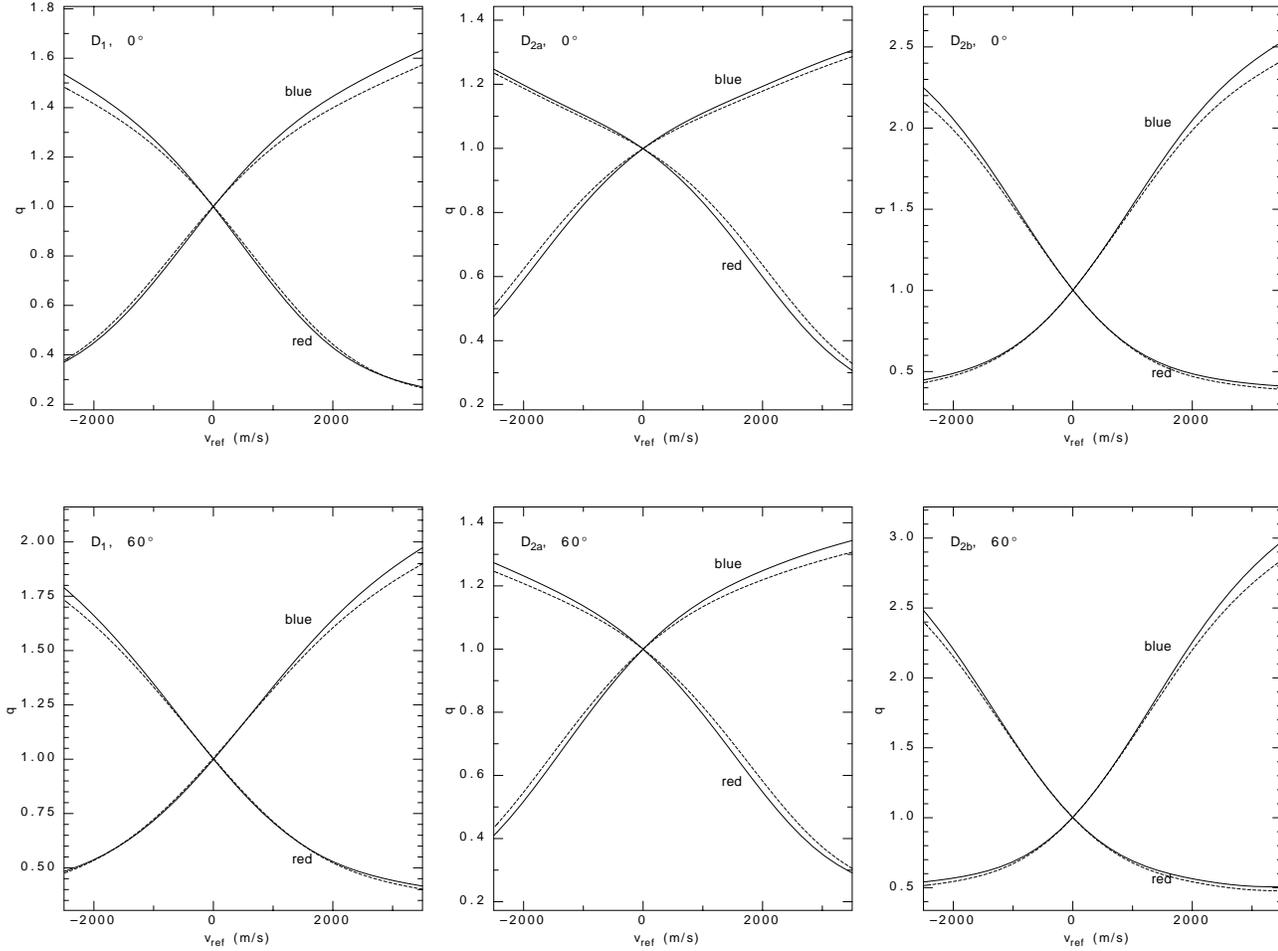so that the intensity can be written:

Fig. 3. The line profile ratio functions needed to determine the local intensity as a function of the local reference velocity v_{ref}. The solid lines and dashed lines are for the − and + states of magnetic modulation respectively. When each of these quantities is multiplied by a line bisector intensity, the result is the local intensity as a function of the offset velocity calculated from the local bisector wavelength.

$$I_b^{\pm}(\rho, v_{\text{ref}}) = \sum_i \phi_i \, I_{\Delta_i^{\pm}}(\rho) \, q_{i,b,\Delta_i^{\pm}}(v_{\text{ref}}) \tag{20}$$

$$I_r^{\pm}(\rho, v_{\text{ref}}) = \sum_i \phi_i \, I_{\Delta_i^{\pm}}(\rho) \, q_{i,r,\Delta_i^{\pm}}(v_{\text{ref}}) \,. \tag{21}$$

The q functions are shown in Fig. 3.

The task of calculating the intensity now consists of two parts: a determination of $v_{\text{ref}}(x,y)$ and a determination of the limb darkening function. Ideally we would use observations in both the D lines to obtain these functions. In fact, the difficulty with telluric contamination prevents the use of any magnetogram data for the D_2 component. For this line the D_1 limb darkening law has been adopted by rescaling to the level indicated by disk center line profiles. In addition, the extensive database at the Mt. Wilson 150-foot solar tower of observations of solar rotation and large scale velocities using the FeI line at $\lambda 525.0$ nm makes it desireable to base the surface velocity patterns on this system.

Turning first to the reference velocity, we can identify four parts: the gravitational redshift $V_{\text{grav.}}$, the sun-spacecraft velocity V_{orbit}, a convective shift $V_{\text{conv.}}$ and a relative surface velocity $V(x,y) = v(x,y) - v(0,0)$. Although the last two of

these velocities may in fact depend on the bisector choice, at the moment we neglect this effect since we do not have adequate data to determine these shifts. The disk center reference velocity $v_{\text{ref}}(0,0)$ defines a time dependent offset velocity which is the primary cause of the shift of the GOLF working points across the solar profile:

$$V_{\text{offset}} = v_{\text{ref}}(0,0) = V_{\text{grav.}} + V_{\text{orbit}} + V_{\text{conv.}} \,. \tag{22}$$

The velocity measured by the magnetograph system uses the disk center position as a zero point and provides:

$$\begin{aligned} V(x,y) &= v(x,y) - v(0,0) \\ &= p(x,y)\Omega(x,y) + V_{\text{Limb}} + V_{\text{Merid}} \end{aligned} \tag{23}$$

where $p(x,y)$ is a projection factor and $\Omega(x,y)$ is the synodic rotation rate:

$$p(x,y) = -R_{\odot} \, \sin(\delta\ell) \cos(b) \cos(b_0) \tag{24}$$

$$\Omega(x,y) = \alpha_1 + \alpha_2 \sin^{10}(\delta\ell) - \beta \sin^2(b) - \gamma \sin^4(b) \tag{25}$$

where $\delta\ell$ is the central meridian angle, b is the solar latitude, and b_0 is the observed solar polar axis tilt. The rotation rate parameters α_1, α_2, β and γ are related to the traditional A, B, C

coefficients used by the Mt. Wilson synoptic program. As can be seen from Eqs. (24) and (25) the rotational velocity is expressed in terms of $R_\odot$ for spatial dimensions and Ω for inverse time. Here α_1 is a scattered light corrected synodic equatorial rotation rate which we take to be 2.84 μradian/s and the term with α_2 is mostly related to scattered light but might also include the effects of a vertical gradient in rotation rate. The β and γ parameters are similar to the B and C quantities used by Howard et al. (1980), LaBonte & Howard (1982), Ulrich et al. (1988). However, these parameters are now given different designations to indicate that they are no longer variable and that the structure of the representation equations is now slightly different. We now leave these parameters fixed at $(\beta, \gamma) = (0.4100, 0.4189)$ μradians/s. We also find that α_1 and α_2 are correlated with the measured scattered light. However, when the linear relations are extrapolated to zero scattered light, the value of α_2 remains non-zero with a typical value being -0.02 μradians/sec. The limb shift velocity is represented with a power series having the form:

$$V_{\text{Limb}} = a_1 X + a_3 X^3 + a_4 X^4 \tag{26}$$

where

$$X = 1 - \cos(\rho) \tag{27}$$

and the values of (a_1, a_3, a_4) are $(142, 190, -290)$ m/s. The meridional circulation velocity is given by:

$$V_{\text{Merid.}} = \Big(-28.7 \sin(b) + 35.2 \sin(2b) \Big) \text{ (m/s)} \times$$
$$\Big(\cos(\delta\ell) \sin(b) \cos(b_0) - \cos(b) \sin(b_0) \Big) . \tag{28}$$

Although the above detailed velocity functions have been derived from observations of λ525.0nm, the magnetograms available using the D_1 are consistent with these functions.

The limb darkening function is

$$L_{\Delta_i^\pm}(\rho) = I_{\Delta_i^\pm}(\rho)/I_{\Delta_i^\pm}(0) \tag{29}$$

where the normalization of the disk center intensity can be left somewhat arbitrary for one of the three scattering components. At disk center the ratios $I_{\Delta_{2a}^\pm}/I_{\Delta_1^\pm}$ and $I_{\Delta_{2b}^\pm}/I_{\Delta_1^\pm}$ are approximately 1.13 and 0.54 respectively. The limb darkening function for D_1 is fit to a form similar to that used above for the limb shift in Eq. (26):

$$L = 1 + L_1 X + L_2 X^2 + L_3 X^3 \tag{30}$$

where $(L_1, L_2, L_3) = (-0.466, -0.06, -0.29)$ and X is defined above in Eq. (27).

5. The sensitivity function

The planned GOLF signal would have involved the ratio $R = (I_b - I_r)/(I_b + I_r)$. In this case the normalization factor $I_{\Delta_1^\pm}(0)$ would have cancelled out. Due to the poor operation of the rotating polarization mechanisms, the GOLF instrument now operates in a single wing and the normalization factor is found by comparison to a temporal average of the returned integrated-sunlight signal. For the purpose of the simulation of the GOLF

signal this average can also be calculated by integrating $I_b^\pm(x,y)$ or $I_r^\pm(x,y)$ over the visible solar disk since we use line profile functions which represent an average of the time-variable profiles. To avoid duplication of formulae which are essentially identical, we replace the subscript b or r with w as a generalized wing designation where w can take on the values b and r. The average intensity is then:

$$\langle I_w^\pm \rangle_{x,y} = (\pi R_\odot^2)^{-1} \int_{\text{surf.}} I_w^\pm(x,y)\, dx\, dy \tag{31}$$

The apparent velocity signal detected by GOLF is then the change in intensity due to a mode distributed over the surface according to $\delta v(x,y)$ relative to the average intensity multiplied by a conversion factor V_{w0}:

$$\delta v_w^\pm = V_{w0} \frac{\delta I_w^\pm}{\langle I_w^\pm \rangle_{x,y}}$$
$$= \frac{V_{w0}}{\langle I_w^\pm \rangle_{x,y}\, \pi R_\odot^2} \int_{\text{surf.}} \big(I_w^\pm(x,y)\big)_v'\, \delta v(x,y)\, dx\, dy \tag{32}$$

We define a sensitivity S to be a function of x and y which when multiplied by the surface velocity $\delta v(x,y)$ and integrated over the visible disk yields the observed change in velocity. Consequently, the integral in Eq. (32) shows that the appropriate definition of the sensitivity function is:

$$S_{v,w}^\pm(x,y) = V_{w0} \frac{\big(I_w^\pm(x,y)\big)_v'}{\langle I_w^\pm \rangle_{x,y}} \tag{33}$$

Due to the presence of three scattering components, the character of the sensitivity functions depends on the resonance cell temperature through the ϕ functions. If a single scattering component were present, the response function would simply be dq/dv. Consequently, it is useful to examine these three functions independently to help anticipate the character of a change which could be caused by a change in the balance between the three scattering strengths. These functions are shown in Fig. 4 in a format similar to that used for Fig. 3. The range of velocity shown in these figures is slightly larger than is seen by the GOLF instrument including the effects of orbital velocity variation and solar rotation. The solar disk center curves for $\rho = 0°$ have a restricted range since they do not involve solar rotation. However, the significant non-linearity shown for the 60° case and which is present at 75° as well, indicates that the representation of the solar line profiles as triangles or trapezoids is not a good approximation. Due to the fact that the signal comes from all three components, some of the slope variation seen in this figure in fact cancels out and the net non-linearity is not as extreme as is shown in this figure.

The velocity conversion factor can be estimated in two ways. The variation in the orbital velocity corresponds to a uniform shift of the whole solar surface, i.e. it is equivalent to picking $\delta v(x,y)$ to be a constant which may arbitrarily be taken as unity. Eq. (32) then yields:

$$V_{w0} = \langle I_w^\pm \rangle_{x,y} \Big/ \Big\langle \big(I_w^\pm(x,y)\big)_v' \Big\rangle_{x,y} . \tag{34}$$
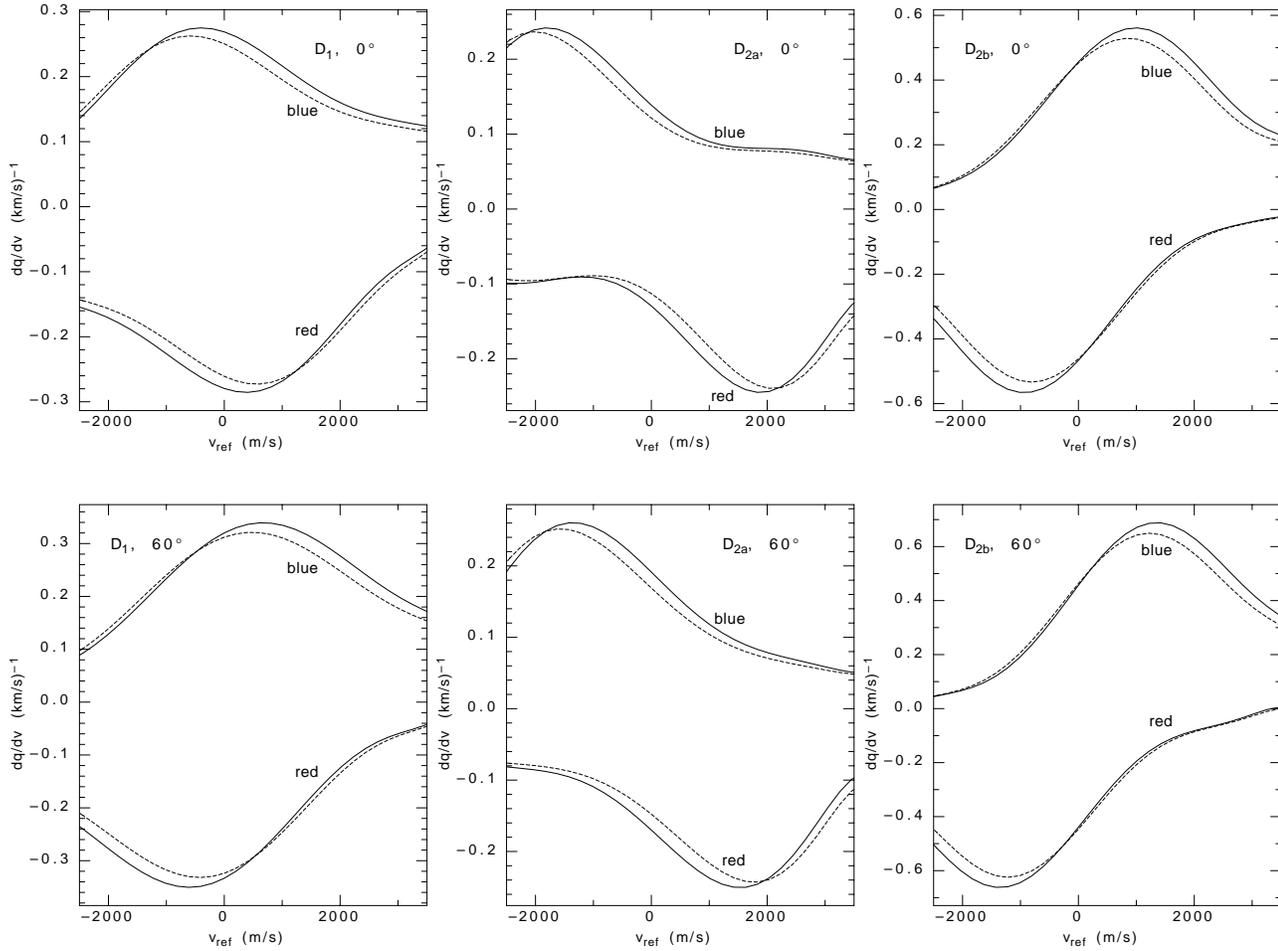
Fig. 4. The sensitivity functions for each of the scattering components. Each of these curves is the local line slope normalized by the local bisector intensity. The velocity is relative to the wavelength of the local line bisector.

The second method is by tracking the observed GOLF output as a function of $V_{\rm orbit}$ and applying the analysis of Ulrich et al. (1998). The comparison is shown in Fig. 5 for two values of cell stem temperature. There are four points of comparison relevant on this figure: the value of V_{b0}, the slope of V_{b0} as a function of $v_{\rm offset}$, the separation between the values of V_{b0}^{+} and V_{b0}^{-} parameterized as $\Delta V_{b0} = (V_{b0}^{+} - V_{b0}^{-})$ and the curvature of V_{b0} as a function of $v_{\rm offset}$. The excellent agreement between all these parameters represents a strong validation of the model. Of these four points of comparison, only the curvature is not well reproduced from the ground-based profile model.

While values for many parameters go into this model, these parameters are all determined from data other than that shown in Fig. 5. Furthermore, we are primarily interested in using spatially resolved data to reproduce the GOLF signal which means that we do not need V_{b0} separately but rather use V_{b0} to convert the GOLF signal to a velocity and at the same time use $S_{vb}^{\pm}(x, y)$ to convert the spatially resolved data to an equivalent GOLF velocity. As long as the model is consistent between these two applications, most uncertainties cancel. The largest uncertainty in the model concerns the treatment of the spectral resolution of the Mt. Wilson system and the effect of line smearing due to spa-
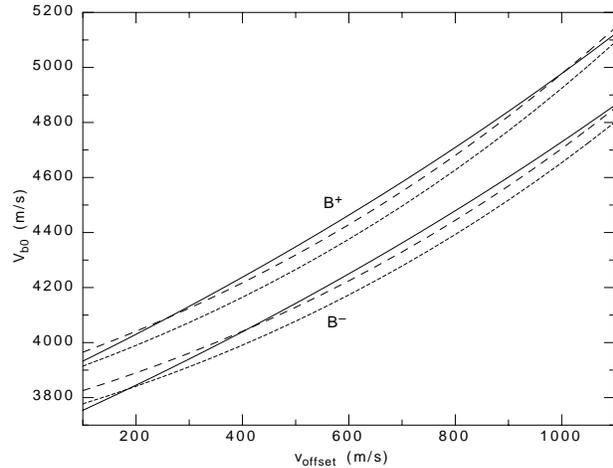

Fig. 5. The conversion factor V_{b0} derived from the GOLF measurements on SOHO shown as the solid lines to the same parameter derived from the ground-based line profiles for two stem temperatures: 146°K (short-dashed lines) and 155°K (long-dashed lines).

tially unresolved line-of-sight velocities. Either of these effects produce changes in the V_{b0} functions at the 5% level and we be-

lieve they cancel so that it is best to adopt the directly observed profiles as we have done here. The scattered light corrections to both GOLF and the Mt. Wilson profiles are constrained respectively by GOLF data taken during cool cell periods and the fit of the core intensity of the Mt. Wilson profiles to those measured by the double-pass system of Delbouille et al. (1973). The values of V_{b0} are changed by 2% when this correction is dropped. The amplitude of magnetic modulation almost exclusively governs the separation between the V_{b0} curves for the two states of modulation. Note that the amplitude of magnetic modulation was adjusted in the paper describing the instrument sensitivity Ulrich et al. (2000) in order to account for the two wing data. The results here also depend on the value adopted in that paper but no further adjustment was made to achieve the agreement shown here.

6. Magnetic field effects

An important additional task is the identification and quantification of the non-coherent magnetically induced signal seen by GOLF. For this purpose we need to use an independent set of information having time resolution in the frequency range of interest but which is derived from spatially resolved and magnetically sensitive measurements such as are available from the MDI experiment. The MDI instrument provides a line depth parameter which indicates the equivalent width of the $\lambda 676.8$nm line and that this parameter is magnetically sensitive. However, it does not provide a definite one-to-one mapping to the magnetic field and is also subject to influence by non-magnetic effects, especially on some portions of the solar image (e.g. Henney et al. 1998) and is available only on a 12 minute cadence after anti-aliasing temporal filtering. In addition, the MDI instrument also provides magnetograms but only once every 90 minutes. Consequently, there is not a single dataset which provides adequate information for use in modeling the magnetic effects on the GOLF data stream. Nonetheless, it may be possible to combine these data streams in such a way as to mitigate the magnetic effects on the GOLF signal. In order to prepare for such analysis, we give here a treatment of the magnetic effects in a form which is consistent with the discussion above of the velocity modelling.

We define sensitivity functions for magnetic field effects in the form:

$$S^{\pm}_{|B|,b}(x,y) = V_{b0} \frac{\left(I^{\pm}_b(x,y)\right)'_{|B|}}{\langle I^{\pm}_b \rangle_{x,y}} \tag{35}$$

$$S^{\pm}_{|B|,r}(x,y) = V_{r0} \frac{\left(I^{\pm}_r(x,y)\right)'_{|B|}}{\langle I^{\pm}_r \rangle_{x,y}} . \tag{36}$$

The key new quantities are the magnetic field derivatives in the numerators of these expressions. These can be written:

$$\left(I^{\pm}_b(x,y)\right)'_{|B|} = \sum_i \phi_i \left[\frac{dI_{\Delta^{\pm}_i}}{d|B|} q_{i,b,\Delta^{\pm}_i} + I_{\Delta^{\pm}_i} \frac{dq_{i,b,\Delta^{\pm}_i}}{d|B|} \right] \tag{37}$$

$$\left(I^{\pm}_r(x,y)\right)'_{|B|} = \sum_i \phi_i \left[\frac{dI_{\Delta^{\pm}_i}}{d|B|} q_{i,r,\Delta^{\pm}_i} + I_{\Delta^{\pm}_i} \frac{dq_{i,r,\Delta^{\pm}_i}}{d|B|} \right] \tag{38}$$

In order to evaluate these expressions and apply them to the case of the GOLF data, it is necessary to have measurements of the magnetic sensitivity of both D lines. Unfortunately, the telluric contamination of the D_2 line compounds the difficulty of isolating magnetic effects on the line profile. As a result a set of resolved sun profile measurements adequate to evaluate the derivatives in Eqs. 37 and 38 is available only for the case of the D_1 profile. Consequently, we are forced to neglect the separate contributions for the D_2 line and assume that the variations in the D_1 line are representative of the total effect on the GOLF instrument. This may be a resonable approach since at the position of the working point on the D_1 line the line shape parameters are intermediate between those of the two working points on the D_2 line. With this approximation we can write:

$$\frac{\left(I^{\pm}_b(x,y)\right)'_{|B|}}{I_{\Delta^{\pm}_1}(0)} = L_{\Delta^{\pm}_1} q_{1,b,\Delta^{\pm}_1} (\gamma_b - G) \tag{39}$$

$$\frac{\left(I^{\pm}_r(x,y)\right)'_{|B|}}{I_{\Delta^{\pm}_1}(0)} = L_{\Delta^{\pm}_1} q_{1,r,\Delta^{\pm}_1} (\gamma_r - G) \tag{40}$$

where the sensitivity coefficients G, γ_b and γ_r are:

$$G = -\frac{d\ln\left(L_{\Delta^{\pm}_1}\right)}{d|B|} \tag{41}$$

$$\gamma_b = \frac{d\ln\left(q_{1,b,\Delta^{\pm}_1}\right)}{d|B|} \tag{42}$$

$$\gamma_r = \frac{d\ln\left(q_{1,r,\Delta^{\pm}_1}\right)}{d|B|} . \tag{43}$$

The response of the D_2 line could be included in similar formulae by replacing these sensitivity coefficients with appropriately weighted averages over the three components.

Two sets of data have been used to evaluate the sensitivity coefficients for the D_1 line. First, during the period from Nov. 1, 1992 to Feb. 3, 1993, a sequence of line scans following the methods described in Sect. 3. These observations lead to a determination of γ_b and γ_r as a function of the velocity relative to the bisector velocity. Second, magnetograms taken in the D_1 line were selected for good sky transparency and good distribution of magnetic activity and used to determine the correlation between bisector intensity and magnetic field strength in annular rings. These observations lead to a determination of G. The magnetograms from 25-Jun-2000 to 28-Jun-2000 along with those from 19, 20 and 24-Jul-2000 were used for the bisector intensity versus magnetic field strength correlation determination. Six annular rings were chosen having center-to-limb angle limits defined by $a_i < \sin \rho < a_{i+1}$ with $a_i = (0.0, 0.3, 0.5, 0.7, 0.85, 0.93, 0.97)$. The magnetograms utilize spectral selection ports having separations of 19.6 and 22.8 pm. The two GOLF bisector half-separations for the D_1 line correspond to 10.72 and 11.09 pm. The correlation
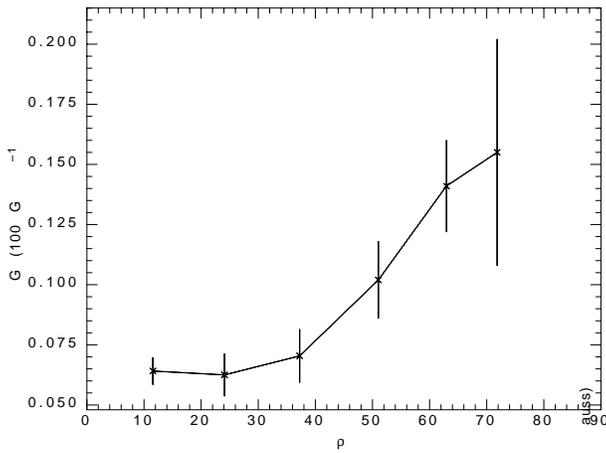
Fig. 6. The dependence of the bisector intensity correlation coefficient on the center-to-limb angle ρ.

Table 1. Line profile observations

Date	$|B|$	ρ	Date	$|B|$	ρ
		Disk	Center		
Low Field			High Field		
30-Dec-92	4.5	0.0	1-Nov-92	214.7	10.4
31-Dec-92	3.6	15.3	2a-Nov-92	200.5	19.3
27-Jan-93	5.8	29.9	2b-Nov-92	182.8	20.9
2-Feb-92	7.5	0.0	4-Nov-92	190.9	35.7
4-Feb-92	7.9	14.9	13-Dec-92	151	27.9
		Mid-Range			
Low Field			High Field		
23-Jan-93	4.6	44.9	10-Nov-92	112.8	47.3
28-Jan-93	0.0	44.8	12-Nov-92	101.6	55.1
			2-Dec-92	94.1	51.0
			10-Dec-92	151.2	50.3
			24-Dec-92	85.7	47.3
		Limb Zone			
Low Field			High Field		
25-Jan-93	0.8	74.9	16-Nov-92	97.3	67.7
29-Jan-93	2.1	59.9	27-Nov-92	112.4	62.9
1-Feb-93	1.8	74.9	15-Dec-92	92.3	66.1
			19-Dec-92	149.7	59.9

coefficients from the magnetograms were interpolated to correspond to 10.90 pm. The derived values of G are shown in Fig. 6. The error bars shown are from the changes between the different magnetograms utilized. The observations used for the line profile sensitivity determination are listed in Table 1. They were averaged in the groups indicated and the changes in the averages were normalized for a 100 gauss magnetic field difference. The derived γ functions are shown in Figs. 7 and 8. Note that because the G and γ functions tend to cancel, the magnetic effect tends to emphasize those parts of the solar disk which are closest to the bisector velocity.

The magnetic darkening process was discussed by Ulrich (1993) and the effect can be modelled in the GOLF data. The present results are consistent with this previous publication and
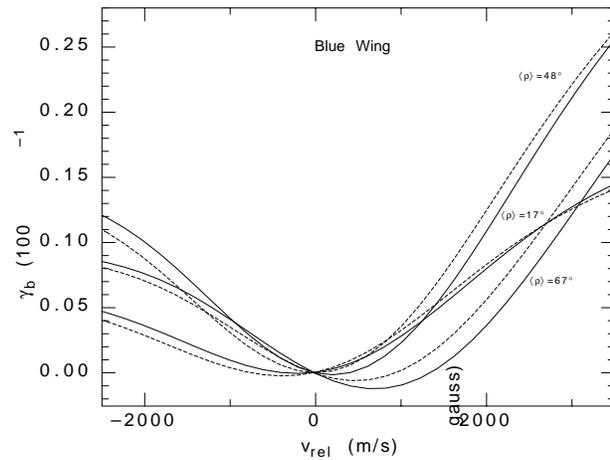

Fig. 7. The dependence of γ_b on the reference velocity (the velocity offset from the bisector point).
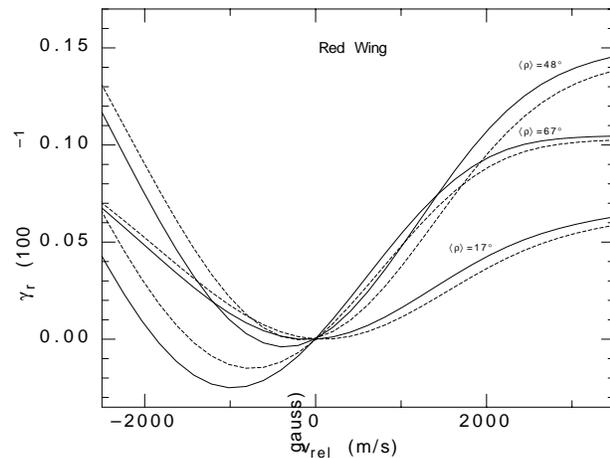

Fig. 8. The dependence of γ_r on the reference velocity.

provide more detail for application to modelling the effect. The MDI instrument provides a proxy based on the shape of the Ni line at $\lambda 676.8$nm. The correspondence between this parameter and the solar magnetic field is not perfect and it may be necessary to combine high temporal cadence information from the line width parameter with lower temporal cadence information from the direct MDI magnetograms. The Mt. Wilson 150-foot solar tower utilizes a 24 channel system which permits the simultaneouos simulation of these MDI parameters - the magnetic field calculated from velocity images taken with opposite states of circular polarization and the line depth parameter I_d along with the measurement of B_{GOLF}, the magnetic field at the GOLF working points in the D_1 line. From this data we estimate that the MDI magnetic field is about 80% as strong as that from the D_1 line and that the derivative $dI_d/d|B_{\mathrm{GOLF}}| \approx 0.04/100$ (gauss)$^{-1}$. For a fixed value of $|B_{\mathrm{GOLF}}|$ the scatter in I_d is about 0.03 so that a simple conversion of I_d to a change in intensity at the GOLF working point could produce a noisy result.

Future instruments such as those under development by the GONG project will provide magnetic field measurements with adequate temporal cadence. Analysis of the shape of the tem-

poral power spectrum of GOLF single-wing data shows that active regions are a major contributor in the frequency range of interest (Ulrich et al. 2000). This result lends urgency to the development of a full treatment of the active region effects.

7. Conclusions

We have presented a model of the GOLF system which allows the calculation of the instrument response to specified spatial velocity functions and given sensitivity functions for use with the evaluation of magnetic field effects. This model requires quantitative values for a number of instrumental parameters including the scattering strengths and the instrument parasite light. The values used are derived from measurements during preflight tests or from an analysis of the data returned from the spacecraft. The comparison shown in the previous section between the model $V_{b0}^{\pm}$ as a function of v_{offset} and the values deduced directly from the GOLF observations provides a critical validation of the chosen parameters.

The approach we have adopted in previously published papers (Henney et al. 1999, Bertello et al. 2000a, 2000b) uses the signal cross-correlation method instead of the signal subtraction method. The cross-correlation approach is much less demanding on the modelling theory than would be the subtraction method. We describe here some of the extensions which would be desireable in an application of the signal subtraction method should future instrument systems provide adequately low-noise data.

The velocity and magnetic field effects discussed in this paper must be joined by effects due to temperature and intensity fluctuations which are part of the oscillatory and convective processes. For the coherent oscillations from the GOLF instrument, this question has been studied by Pallé et al. (1999) and by Renaud et al. (1999). These studies show that for the higher frequency coherent oscillations, the signal due to the thermal or excitation effects in the solar atmosphere produces only small alterations in the phase relationships that one would get from an instrument which measures only velocity. However, the convective and magnetic phenomena which can also contribute to the GOLF single wing signal through the intensity may have a completely different nature. As part of the synoptic program at the 150-foot solar tower on Mt. Wilson, daily intensity images are made available on the web page at `http://www.astro.ucla.edu/~obs/intro.html`. These are line bisector images for both $\lambda 525.0$ and Na D_1. The bisector intensity as shown by these images is clearly altered by the presence of both weak and strong magnetic fields. In addition, outside of the magnetized areas, the intensity shows variations on a spatial scale comparable to the supergranulation or chromospheric network. These features appear to be convective in origin and are probably a component of the low frequency noise which interferes with the search for coherent solar oscillations.

The Mt. Wilson 150-foot solar tower system now includes regular observations of the $\lambda 676.8$nm line in a manner which permits the simulation of the MDI signal. A comparison between images of the MDI line depth parameter and the D_1 bisector intensity suggests that the MDI line depth can be used to derive the convective intensity variations. Efforts to quantify this possibility are currently in progress. The MDI instrument also provides a continuum flux index which can be used to identify sunspot regions and treat their contribution in a different but appropriate manner. Sensitivity functions like those of Eqs. (35) and (36) can be written using a multiple parameters like the MDI line depth and continuum flux observables instead of $|B|$. As long as appropriate coefficients are known to convert these parameters into a resulting line bisector intensity change, the equations can be applied immediately to the simulation. We know from Ulrich et al. (1993) that the primary effect on a resonance scattering cell signal can be modelled. It will require a detailed application to the GOLF data to determine the frequency range of validity of this model.

The inclusion of additional information derived from the available data bases will make it possible to carry out a simulation of the GOLF signal which takes into account a variety of non-coherent solar phenomena. If the simulation is successful, it may be possible to enhance the ratio of coherent oscillation signal relative to the non-coherent contributions and improve the detectability of weak solar oscillations. The MDI instrument has available data products which can be applied to this project: First are two velocity sequences - the medium ℓ velocities which have good spatial resolution and are at the full temporal cadence of MDI but omit data from the solar limb regions and contain some temporal gaps due to the telemetry mode and other programatic factors, and the VIRGO/LOI mask sequence which has lower spatial resolution but includes the limb zone and has better temporal coverage. Second, are two non-velocity measures of the solar surface – the line depth parameter and the continuum flux parameter. Both these are available only in the form of gaussian smoothed temporal averages of 128×128 arrays. The temporal sampling is once every 12 minutes and the temporal smoothing is done over 23 images using a gaussian weight having a standard deviation of 3.4 minutes. One bad image out of the 23 will spoil the telemetered image so this series includes a high number of missing frames. Nonetheless these sequences permit removal of some of the variations detected by GOLF which are produced by identifiable solar processes that are not coherent oscillations.

and Instituto de Astrofísica de Canarias, Tenerife, Spain. These institutes are supported by a large number of scientific Co-Investigators drawn from many countries. SOHO is a mission of international cooperation between ESA and NASA.

References

Babcock H.W., 1953, Astrophys. J. 118, 387

Bertello L., Henney C.J., Ulrich R.K., et al. , 2000a, ApJ 535, 1066

Bertello L., Varadi F., Ulrich R.K., et al. , 2000b, Astrophys. J. Letters 537, L143

Boumier P., 1991, *PhD Thesis* University of Paris VII

Boumier P., Damé L., 1993, Expimental Astron. 4, 87

Christensen-Dalsgaard J., 1989, Monthly Notices Roy. Astron. Soc. 239, 977

Delbouille L., Roland G., Neven L., 1973, *Photometric Atlas of the Solar Spectrum* Inst. d' Astrophysique; Univ. Liège

Gabriel A.H., Grec G., Charra J., et al. , 1995, Solar Phys. 162, 61

Gabriel A.H., Charra J., Grec G., et al. , 1997, Solar Phys. 175, 207

García R.A., Roca Cortés T., Régulo C., 1998, A&A Suppl. 128, 389

García R.A., Turck-Chièze S., Robillot J.-M., et al. , 2000, A&A in preparation

Henney C.J., Bertello L., Ulrich R.K., et al. , 1998, In: Korzennik S., Wilson A. (eds.), (ESA Publications: Noordwijk), p. 219

Henney C.J., Ulrich R.K., Bogart R.S., et al. , 1998, In: Provost J., Schmider F.X. (eds.), (Observatoire de la Côte d'Azur et Universite de Nice: Nice, Fr.), p. 179

Henney, C.J., Ulrich, R.K., Bertello, L., et al. , 1999, A&A 348, 627

Henney, C.J., 1999, *PhD Thesis* University of California at Los Angeles

Howard R., Boyden J.E., LaBonte B.J., 1980, Solar Phys. 66, 167

LaBonte B.J., Howard R., 1982, Solar Phys. 80, 361

Pallé P.L., Régulo C., Roca Cortés T., et al. , 1999, A&A 341, 625

Reader J., Corliss C.H., 1980, *Wavelengths and Transition Probabilities for Atoms and Atomic Ions – Part I. Wavelengths* US-NBS: US Gov. Printing Office, Washington DC

Renaud C., Grec G., Boumier P., et al. , 1999, A&A 345, 1019

Robillot J.-M., Turck-Chièze S., García, R.A., et al. , 1998, In: Korzennik S., Wilson A. (eds.), (ESA Publications: Noordwijk), p. 317

Ulrich R.K., Boyden J.E., Webster L. et al. , 1988, Solar Phys. 117, 291

Ulrich R.K., Webster L., Boyden J.E. et al. , 1991, Solar Phys. 135, 211

Ulrich R.K., Henney C.J., Schimpf S., et al. , 1993, A&A 280, 268

Ulrich R.K., García R.A., Robillot J.-M., et al. , 1998, In: Korzennik S., Wilson A. (eds.), (ESA Publications: Noordwijk), p. 353

Ulrich R.K., García R.A., Robillot, J.-M. et al. , 2000, A&A in press